

AD-A103 533

NAVAL RESEARCH LAB WASHINGTON DC  
ELIMINATION OF SHORT PULSE INTERFERENCE IN PULSE COMPRESSION RA-ETC(U)  
SEP 81 J D WILSON  
NRL-8567

F/6 17/0

ML

UNCLASSIFIED

10/1  
A  
AD-8567

END  
DATE  
FILED  
40-81  
OTIC

LEVEL

12

NRL Report 8507

AD A103533

## Elimination of Short Pulse Interference in Pulse Compression Radars

J. D. WILSON

Radar Analysis Branch  
Radar Division

September 3, 1981



NAVAL RESEARCH LABORATORY  
Washington, D.C.

Approved for public release; distribution unlimited.

31 0 01 053

FILE COPY

SECURITY CLASSIFICATION OF THIS PAGE (When Data Entered)

(11) RJD-105

REPORT DOCUMENTATION PAGE		READ INSTRUCTIONS BEFORE COMPLETING FORM
1. REPORT NUMBER NRL Report 8507	2. GOVT ACCESSION NO. AD-A103533	3. RECIPIENT'S CATALOG NUMBER
4. TITLE (and Subtitle) <u>ELIMINATION OF SHORT PULSE INTERFERENCE IN PULSE COMPRESSION RADARS</u>	5. TYPE OF REPORT & PERIOD COVERED Interim report on a continuing NRL problem	
6. AUTHOR(s) J. D. Wilson	7. CONTRACT OR GRANT NUMBER(s)	
8. PERFORMING ORGANIZATION NAME AND ADDRESS Naval Research Laboratory Washington, DC 20375	9. PROGRAM ELEMENT, PROJECT, TASK AREA & WORK UNIT NUMBERS 61153N RR0210541 NRL Problem 53-0628-0	
10. CONTROLLING OFFICE NAME AND ADDRESS Naval Research Laboratory Office of Naval Research Washington, DC 20375	11. REPORT DATE 3 September 1981	
12. MONITORING AGENCY NAME & ADDRESS (if different from Controlling Office) 13. NUMBER OF PAGES 14	13. NUMBER OF PAGES 14	
15. SECURITY CLASS. (of this report) UNCLASSIFIED	16. DECLASSIFICATION/DOWNGRADING SCHEDULE	
17. DISTRIBUTION STATEMENT (of this Report) Approved for public release; distribution unlimited.		
18. DISTRIBUTION STATEMENT (of the abstract entered in Block 20, if different from Report) 14 NKL-8507		
19. SUPPLEMENTARY NOTES		
20. ABSTRACT (Continue on reverse side if necessary and identify by block number) Preliminary to a study on environmental mapping based on real data, a simulation was developed to study short pulse interference and its effect on detection in a pulse compression radar. A simulation was needed because the available data were recorded after the pulse compression network. This is too late to eliminate short pulse interference; it must be detected and eliminated prior to pulse compression. The simulation also treats the problem of removing clutter and short pulse interference when both are present. The simulation involved a signal of approximately the same level as the noise, short pulse interference peaking 40 dB above the noise, and clutter with average level the same as the peak level		
		(Continues)

20. Abstract (Continued)

of the short pulse interference. With these levels, either short pulse interference or clutter would inhibit detection, but prepulse compression blanking of the interference and postpulse compression cancellation of the clutter allowed detection of the target signal.

X

## CONTENTS

INTRODUCTION .....	1
SIMULATION OF TARGETS .....	1
DESCRIPTION OF FILTERS .....	2
APPLICATION OF FILTER WEIGHTING .....	2
GENERATION OF NOISE .....	3
DESCRIPTION OF SHORT PULSE INTERFERENCE .....	4
DESCRIPTION OF DOPPLER .....	4
DETECTION OF SHORT PULSE INTERFERENCE .....	6
GENERATION OF CLUTTER .....	7
DETECTION OF TARGETS .....	8
SUMMARY .....	10
REFERENCES .....	11

Accession For NTIS GEN&I DTIC T-3 Unannounced Justification	<input checked="" type="checkbox"/>	<input type="checkbox"/>	<input type="checkbox"/>
By _____			
Distribution/			
Availability Codes			
Printed and/or Dist. by Special			

A

## ELIMINATION OF SHORT PULSE INTERFERENCE IN PULSE COMPRESSION RADARS

### INTRODUCTION

The Radar Division of NRL is currently studying environmental mapping from the viewpoint of improving automatic detection, tracking, and radar control processes [1]. An important factor in this study is the availability of data from a coherent pulse compression system. This radar is broadband with coherent processing and pulse compression. The data recorded will be  $I$  and  $Q$ -channel voltages after pulse compression. This means that one environmental factor we cannot examine in these data is short pulse interference because the pulse compression filter spreads this signal in time by the uncompressed pulse width. This report describes an analysis of this phenomena by simulating the operation of the signal processing hardware [2] on the computer-generated radar signals. The principal features of the simulation will be (1) simulating radar returns, (2) simulating a pulse compression network, (3) performing MTI cancelling, and (4) performing CFAR detection.

Basically, the simulation was developed in the following manner. First, a linear FM target return was generated and passed through a pulse compression network. The next step was to place a Hamming weighting function on the filter and observe the effect of this on the sidelobes of the compressed pulse. These features were examined by plotting these functions. The plots generated are discussed in greater detail in a following section. The next step was to add noise to the waveform. The ratio between target and noise was set to yield a 25 dB signal to noise ( $S/N$ ) ratio after passing through the pulse compression network. Then, short pulse interference (SPI) was added to the signal. The level of the SPI was set 40 dB higher than the average noise. The next major development was a loop to generate two sequential PRFs (one with SPI, one without) which required simulating the Doppler shift of the target, and the mechanism to detect the SPI. Since this was a simulation, the software used to detect the SPI can also be used as part of an MTI used for detection after pulse compressions. Ground clutter set at the same amplitude as the SP. was generated to test the MTI.

### SIMULATION OF TARGETS

The waveform generated was one achievable by an L-band surveillance radar with pulse compression. The waveform was simulated at baseband because of the large number of samples required to obtain a faithful representation of the signal at IF or RF.

The return from an isolated point target was generated from the following expressions for the in-phase  $X_I(t)$  and quadrature-phase  $X_Q(t)$  signals

$$\begin{aligned} X_I(t) &= A \cos\left(\frac{\mu t^2}{2} - \frac{\mu Tt}{2} + \varphi\right), \text{ and} \\ X_Q(t) &= -A \sin\left(\frac{\mu t^2}{2} - \frac{\mu Tt}{2} + \varphi\right), \end{aligned} \quad (1)$$

Manuscript submitted May 17, 1981.

## WILSON

where

$$\begin{aligned} T &= 120 \mu\text{s}, \text{ the uncompressed pulse length,} \\ \mu &= 2\pi/(T\tau), \\ \pi &= 3.14159, \\ \tau &= 0.5 \mu\text{s}, \text{ the compressed pulse length,} \\ \varphi &= \pi/4, \text{ an arbitrary phase term, and} \\ A &= \text{signal amplitude.} \end{aligned}$$

These functions are sampled over the uncompressed pulse length of  $T$  at points  $\Delta t$  apart where  $\Delta t = \tau/4$ .

### DESCRIPTION OF FILTERS

The matched pulse compression filter (PCF) for the waveform described in Eq. (1) is equivalent to a correlation receiver which correlates the received waveform with the complex conjugate of the transmitted waveform. This complex conjugate is given by

$$\begin{aligned} F_{MI}(t) &= \cos\left(\frac{\mu t^2}{2} - \frac{\mu T t}{2}\right) \\ F_{MQ}(t) &= \sin\left(\frac{\mu t^2}{2} - \frac{\mu T t}{2}\right). \end{aligned} \quad (2)$$

The effect of passing the returned waveform through this filter is described by

$$\begin{aligned} Y_I(t) &= X_I(t) * F_{MI}(t) + X_Q(t) * F_{MQ}(t) \\ Y_Q(t) &= -X_Q(t) * F_{MI}(t) + X_I(t) * F_{MQ}(t), \end{aligned} \quad (3)$$

where  $X^*F$  is the cross correlation of  $X$  and  $F$ , i.e.,

$$Y(t) = \int_u X(u-t)F(u) du$$

and the asterisk represents the conjugate. The function  $Z(t) = Y_I(t)^2 + Y_Q(t)^2$  is plotted in Fig. 1 in dB form relative to the largest value.

### APPLICATION OF FILTER WEIGHTING

To achieve better sidelobe levels from the PCF, a Hamming weighting function was generated from

$$W(t) = A_h + (1 - A_h) \cos\left(2\pi \frac{t - T/2}{T}\right), \quad (4)$$

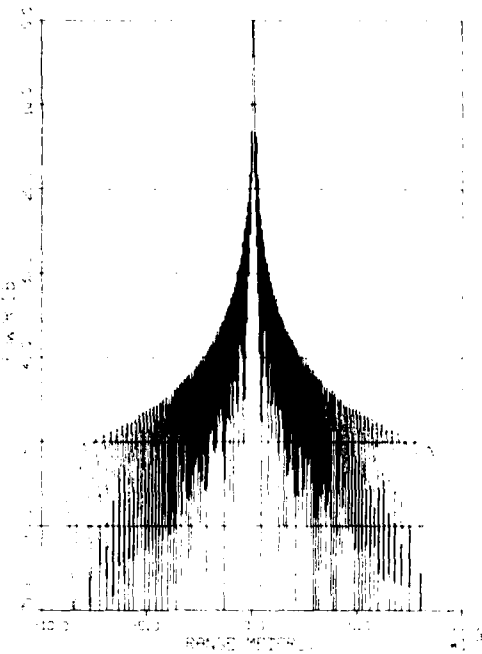


Fig. 1 — Response of unweighted pulse compression filter to a noise-free target signal

where  $A_h = 0.54$ , and applied to Eq. (2) to obtain

$$F_I(t) = W(t) \cos\left(\frac{\mu t^2}{2} - \frac{\mu Tt}{2}\right)$$

and

$$F_Q(t) = W(t) \sin\left(\frac{\mu t^2}{2} - \frac{\mu Tt}{2}\right),$$

which will be used as the pulse compression filter from now on. The result of operating on the signal of Eq. (1) in a manner analogous to Eq. (3) is shown in Fig. 2. While the main beam is broadened, the first sidelobe is lowered nearly 30 dB.

#### GENERATION OF NOISE

Gaussian distributed noise samples may be generated from uniformly distributed random numbers by the relationship

$$G_I = \sigma \sqrt{-2 \log(U_1)} \cos(2\pi U_2), \quad (5a)$$

where  $\sigma$  is the standard deviation desired and  $U_1$  and  $U_2$  are random numbers uniformly distributed on the (0,1) interval. An independent Gaussian variable can be generated from the same two random numbers by

$$G_Q = \sigma \sqrt{-2 \log(U_1)} \sin(2\pi U_2). \quad (5b)$$

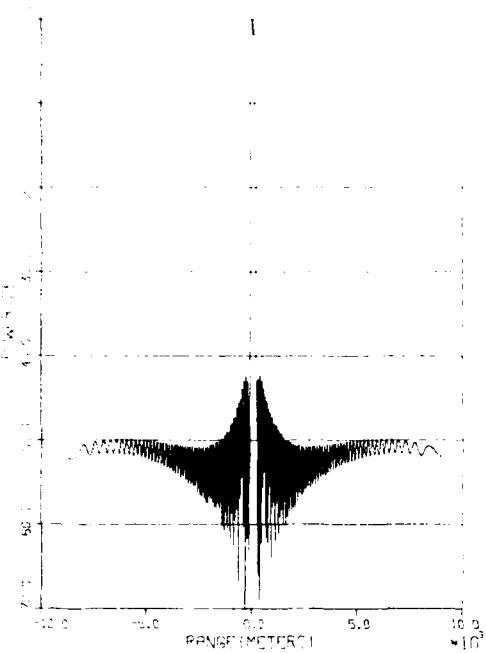


Fig. 2 — Response of a Hamming weighted pulse compression filter to a noise-free target signal

Adding these Gaussian noise terms to the waveform of Eq. (1), and setting  $A$  (of Eq. (1)) to 0.91287 and  $\sigma$  (of noise) to 1.0, we generate a postpulse compression S/N of approximately 25 dB. This ratio was observed by passing signal alone (Eq. (1)) through the filter and then by passing noise alone (Eq. (5)) through the filter. The waveform consisting of signal plus noise prior to filtering is plotted in Fig. 3, and the result of passing the waveform through the filter is shown in Fig. 4.

#### DESCRIPTION OF SHORT PULSE INTERFERENCE

Short pulse interference (SPI) was assumed to be of  $2 \mu\text{s}$  duration and arbitrarily placed about 1/3 of the way through the  $120 \mu\text{s}$  pulse. This pulse length, which is approximately equivalent to a radar range extent of 305 m (1000 ft), was chosen as typical of long-range surveillance radars. The SPI was set 40 dB above the noise level. The waveform of the signal plus noise plus interference is plotted in dB form in Fig. 5, and the response of the filter is shown in Fig. 6.

#### DESCRIPTION OF DOPPLER

The next step is to generate sequential pulses to detect the presence of short pulse interference. (Unless the interfering source has exactly the same pulse repetition frequency or multiple thereof, the interference will not occur at the same range in each pulse.) At this time it was also decided to include the effect of target velocity on the returned waveform. The Doppler component of phase shift of the waveform is given by

$$P_d(t) = \frac{4\pi V_t f_o}{c \text{ prf}} + \psi_o , \quad (6)$$

NRL REPORT 8507

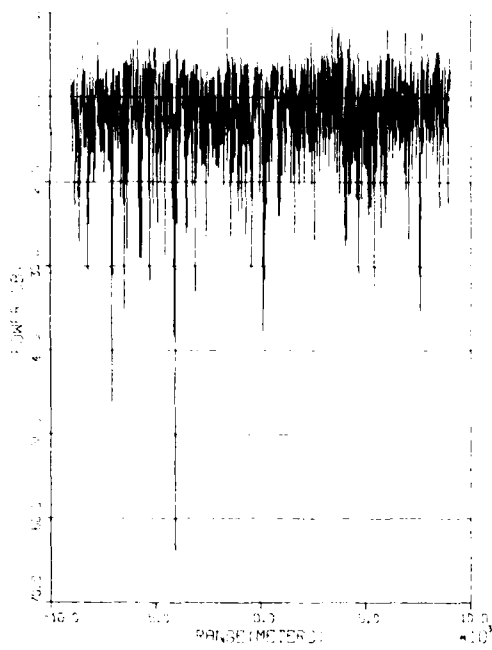


Fig. 3 — Typical target signal plus noise before pulse compression

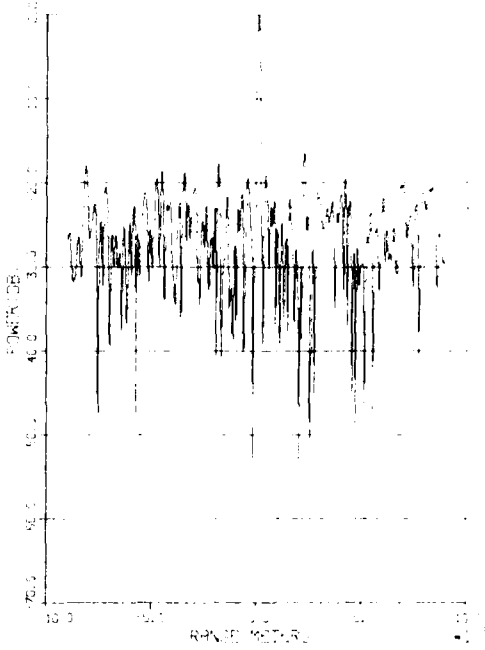


Fig. 4 — Response of a Hamming weighted pulse compression filter to a target signal plus noise

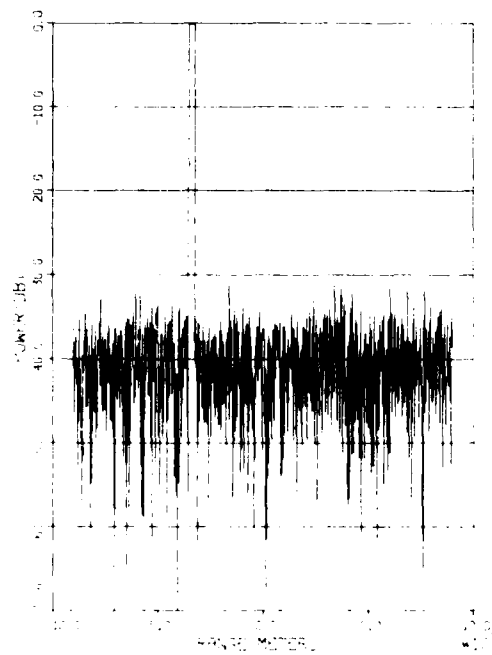


Fig. 5 — Typical target signal plus noise plus interference before pulse compression

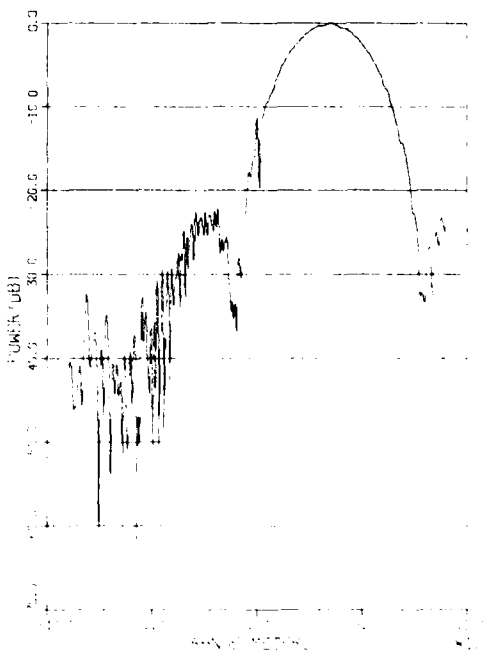


Fig. 6 — Response of pulse compression filter to target signal plus noise plus interference

## WILSON

where

$$V_t \approx 475 \text{ m/s}$$

$$f_o = 1000 \text{ MHz, carrier frequency}$$

$$c = 300 \times 10^6 \text{ m/s, speed of electromagnetic propagation}$$

$$\text{prf} = 333 \text{ pps, pulse repetition frequency}$$

$$\psi_o = \text{portion of phase which is time independent.}$$

We may ignore  $\psi_o$  because it can be absorbed into the general arbitrary phase term  $\varphi$  of Eq. (1).

### DETECTION OF SHORT PULSE INTERFERENCE

To detect short pulse interference, two small routines were generated. The first routine takes the sample by sample difference between two digitized functions. The second routine performs a CFAR detection operation on a digitized function. The CFAR senses the environment and sets a detection threshold based on the mean and standard deviation of the signal in a region where the test for a detection is taking place. Specifically, the samples in a range interval about the sample to be tested are used to estimate the mean and standard deviation with the samples immediately around the test cells ignored. For detecting short pulse interference, first the  $I$ - and  $Q$ -channel voltages of pulse two are subtracted from the  $I$ - and  $Q$ -channel voltages of pulse one and then the envelope of the difference is formed. This coherent subtraction is not necessary; in fact, there are valid reasons for performing the process on the amplitudes of the pulses. However, this is what was done, and the envelope is described by Eq. (7).

$$E(t) = \sqrt{\left[ X_I(t,1) - X_I(t,2) \right]^2 + \left[ X_Q(t,1) - X_Q(t,2) \right]^2}. \quad (7)$$

This envelope is passed through the detector with each sample being tested. Sixteen samples on each side of the test sample are ignored, and the next 32 samples on each side of the test cell are used for reference. Sixteen samples were blanked because that was the expected maximum length of the short pulse interference. If longer pulses were expected, then more samples would have to be blanked to keep the signal we are trying to detect from contaminating the reference cells. The trade-off is that we wish to keep the reference cells as representative of the neighborhood of the test cell as possible, but the reference samples must not be contaminated by signals which extend in range.

The threshold is set with the formula

$$T = m_e + K\sigma_e, \quad (8)$$

where  $m_e$  is the estimated mean level of the environment, and  $K$  is the number of estimated standard deviations,  $\sigma_e$ , of the environment necessary to ensure a given probability of false alarm,  $P_{fa}$ . To determine  $K$ , the distribution of the environment was assumed to be Rayleigh (as it would be for envelope detected independent noise samples), and

$$P_{fa} = \int_T^\infty \frac{X}{\sigma^2} \exp -\frac{X^2}{2\sigma^2} dx \quad (9)$$

was solved for  $T$ , where  $\sigma$  is the standard deviation (s.d.) of the underlying Gaussian. This yields the equation

$$T = \sigma \sqrt{2 \log(1/P_{fa})}. \quad (10)$$

The mean and s.d. of a Rayleigh distribution are related to the s.d. of the underlying Gaussian by

$$\begin{aligned} m_r &= \sigma \sqrt{\frac{\pi}{2}} \\ \sigma_r &= \sigma \sqrt{2 - \frac{\pi}{2}}. \end{aligned} \quad (11)$$

Substituting Eq. (11) into Eq. (8) for the estimated values of the Rayleigh, we obtain

$$T = \sigma \sqrt{\frac{\pi}{2} + K\sigma} \sqrt{2 - \frac{\pi}{2}}. \quad (12)$$

Solving Eqs. (12) and (10) simultaneously we find that  $\sigma$  can be factored out leaving

$$K = \frac{\sqrt{2 \log(1/P_{fa})} - \sqrt{\frac{\pi}{2}}}{\sqrt{2 - \frac{\pi}{2}}}. \quad (13)$$

For a typical value of  $P_{fa}$  of  $10^{-6}$ , we find  $K = 6.11$ . This  $K$  value will actually yield a  $P_{fa} > 10^{-6}$  since the calculation of  $K$  contains the assumption that the estimates are the true values.

With the large interference to noise level quoted (40 dB), the interference was easy to detect. It is expected that if the interference level were low enough that it could not be detected, then after the energy in the short pulse was spread over the entire range interval by passing through the pulse compression filter, then it would be too small compared to the range compressed target pulse to cause any serious problem. Once the samples which contain interference have been determined, these samples are blanked in both pulses. Both pulses are blanked because we intend to use pulse to pulse coherent processing later. The response of the filter to the signal waveform when interference is present but blanked is shown in Fig. 7. Close examination of Figs. 7 and 4 (when interference was not present) reveals only minor differences, indicating that blanking 2  $\mu$ s of a 120  $\mu$ s record has little effect on the filter response. The difference in dB levels in Figs. 7 and 4 reflects only the fact that the dB values are relative to different reference values in each case.

## GENERATION OF CLUTTER

The clutter simulated in the model is ground clutter because the relatively low PRF (333 pps) of the system cannot cancel clutter with larger Doppler spreads such as rain clutter. The clutter return was simulated by taking a large number (in our case, 20) of point targets with random ranges (in the vicinity of the true target), random Dopplers (between  $\pm 0.1$  m/s) and random phases. The amplitude is set to yield an average clutter value equal to the short pulse interference value. The

WILSON

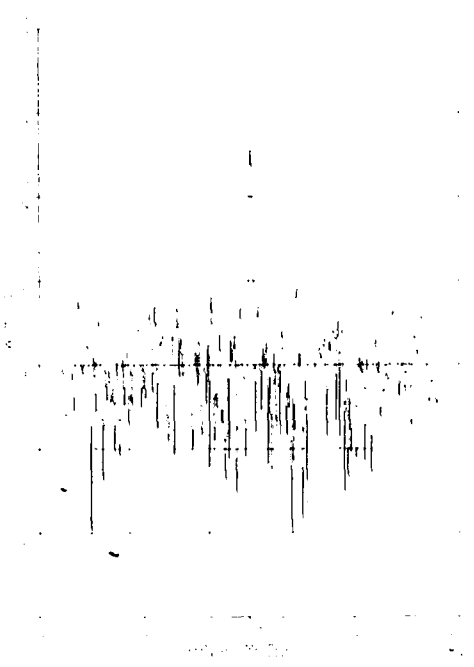


Fig. 7 — Response of pulse compression filter to target signal plus noise plus interference with interference blanked

waveform consisting of target return, noise, interference, and clutter for one pulse is shown in Fig. 8. The second pulse without the interference is practically identical because the noise and target levels are so far below the clutter, the clutter decorrelates very little pulse to pulse, and the interference on the same level as the clutter occupies such a small portion of the pulse. The basic similarity between the pulses is shown in Fig. 9 which shows the envelope discussed earlier in Eq. (7), i.e., the difference of pulses one and two. Comparing Fig. 9 to Fig. 5, we obtain an estimate of the clutter residue of the MTI, and there is roughly a 6 dB difference in interference to noise level in the two figures. If 3 dB of the difference is the result of processing the noise through the MTI, then the clutter residue is 3 dB above the noise. The original clutter level was approximately 40 dB above the noise.

The operation of the filter on the waveform of Fig. 8 is shown in Fig. 10. We know from Fig. 6 that the interference can mask the signal, and now we see that clutter even covers up the distinctive interference. If we take the range filter output of both pulses and pass them through the MTI, we see that the clutter cancels and we now observe the response to the short pulse interference, Fig. 11.

We now have all the types of signals simulated that we set out to simulate and all the processing tools necessary to operate on these signals.

#### DETECTION OF TARGETS

There are two detection processes we could use on two pulses. The first is a coincidence detector based on two pulses. The other is a coherent process using the MTI.

Using the coincidence detector, we assumed a noise only environment with no clutter and no SPI. Since we assume we are detecting in a noisy environment, the probability of false alarm is independent pulse to pulse and we may attain a  $P_{fa}$  of  $10^{-6}$  by setting the threshold to achieve

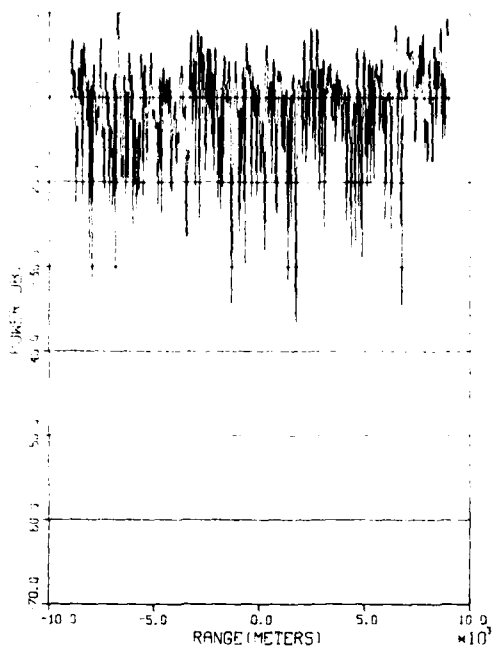


**Fig. 8 — Target signal plus noise plus interference plus clutter before pulse compression**

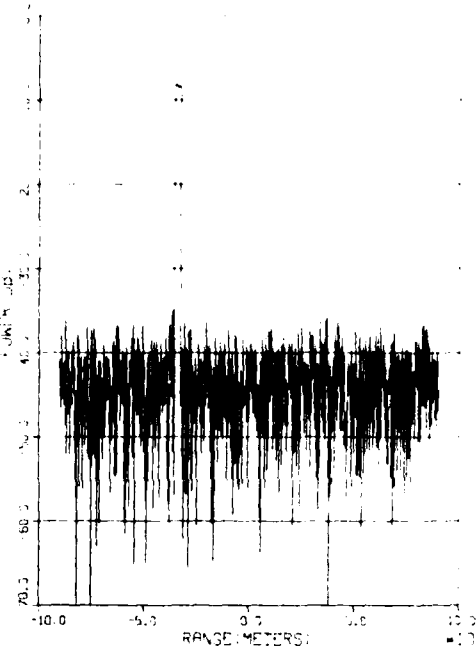


**Fig. 9 — Difference between pulse containing target, noise, interference and clutter and next pulse containing target, noise, and clutter but no interference before pulse compression**

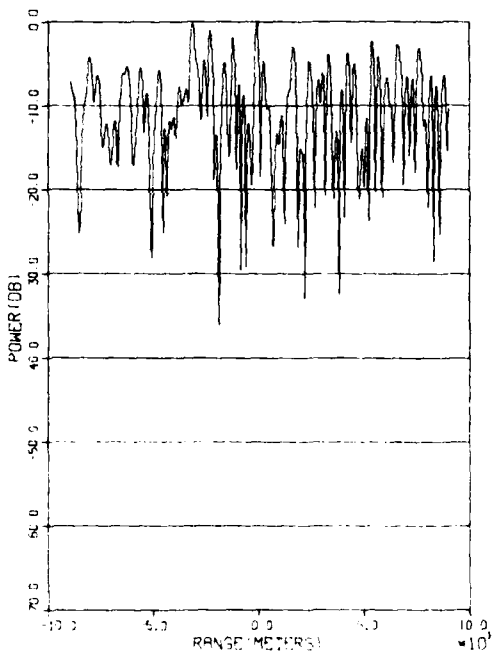


**Fig. 10 — Response of pulse compression filter to signal plus noise plus interference plus clutter (Fig. 8)**

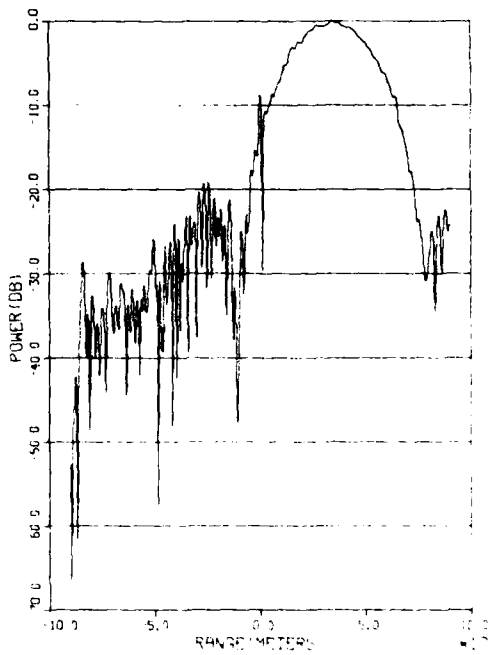


**Fig. 11 — Difference in pulse compression filter response to a pulse including interference and the response to a pulse without interference**

## WILSON

a  $P_{fa}$  of  $10^{-3}$  on each pulse. This is approximated by a value of  $K = 3.76$  in Eq. (8). This detector detects signals in a noisy environment but is the wrong detector in a clutter environment. Since the clutter changes very little from pulse to pulse, a sample which exceeds the threshold on pulse one has very high probability of exceeding the threshold on pulse two. The detections are not independent events. It would be very hard to determine the proper threshold without using Monte Carlo simulations, so we will assume perfect correlation of the clutter pulse to pulse which means to obtain a coincident  $P_{fa}$  of  $10^{-6}$  we set the threshold for each pulse to the value of  $10^{-6}$ . In this case there are no false alarms, but there are no detections.

In the coherent detection process we may first detect the presence of SPI and eliminate it from our uncompressed pulses. Each pulse is then passed through the pulse compression filter to obtain the results shown in Fig. 12. This is virtually indistinguishable from Fig. 10, showing the dominance of the clutter over the SPI. Operating on the two compressed pulses with the MTI yields the results in Fig. 13. The target is easily detectable over the clutter residue, and the effect of blanking the interference is negligible.

## SUMMARY

We have seen that short pulse interference (SPI) has an adverse effect on pulse compression networks. However, we have shown that SPI can be eliminated by subtracting two successive pulses prior to pulse compression. This has the effect of eliminating clutter, if present, and highlighting the SPI which would appear in at most one of the pulses. The SPI can then be eliminated by blanking the cell in which it appears and then continuing processing in a normal manner. This would include postpulse compression detection of targets either coherently or noncoherently depending on the presence or absence of clutter. Blanking the few cells occupied by the SPI seemed to have

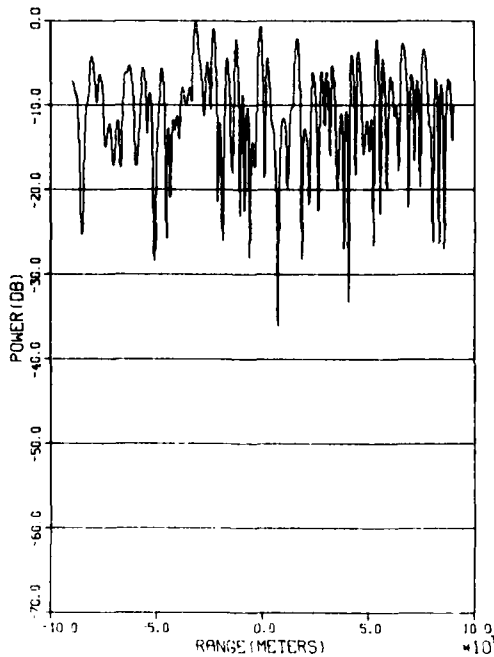


**Fig. 12 — Response of pulse compression filter to signal plus noise plus interference plus clutter with interference blanked**

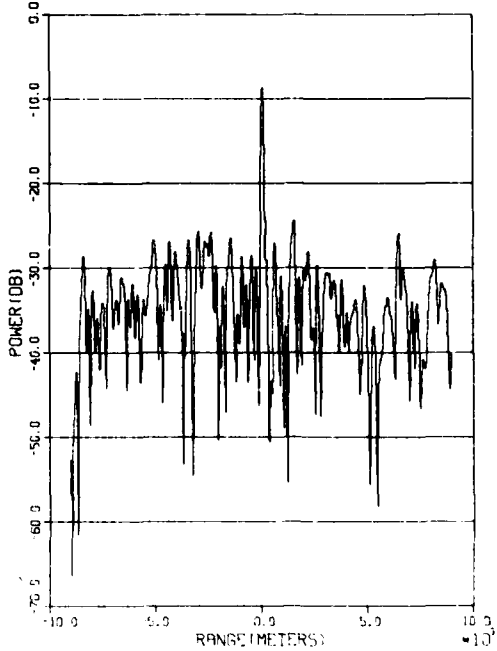


**Fig. 13 — Difference of pulse compression filter responses to two pulses where interference is blanked prior to filtering**

NRL REPORT 8507

little effect on the total information content of the long pulse. In the absence of SPI, no cells would be blanked if the threshold of the interference detector is set properly.

This seems to be a promising means of extracting targets buried in noise, short pulse interference, and/or clutter, and we hope to consider ways of implementing it in radars in the future.

REFERENCES

1. B. H. Cantrell, "Preliminary Results of Radar Environmental Mapping," NRL Report 8400, April 28, 1980.
2. B. Lewis and F. Kretschmer, "Interference Suppressor Radar MTI," Navy Case No. 64,619.